Int. J. Environ. Sci. Technol. (2016) 13:147–158
DOI 10.1007/s13762-015-0854-6

ORIGINAL PAPER

Degradation of Acid Blue 161 by Fenton and photo-Fenton processes

A. G. Trovó[1] **· A. K. Hassan**[2] **· M. Sillanpää**[3] **· W. Z. Tang**[4]

Received: 20 June 2014 / Revised: 9 April 2015 / Accepted: 6 July 2015 / Published online: 22 July 2015

Abstract Degradation kinetics of azo dye, Acid Blue 161 (AB161), by Fenton and photo-Fenton processes in aqueous solution was investigated. At pH 3.5, the effects of H_2O_2, Fe^{2+}, and H_2O_2/Fe^{2+} molar ratios, on the AB161 decolorization kinetic rates, were evaluated. Experimental results confirmed that the optimal H_2O_2/Fe^{2+} molar ratio of 12 is close to the theoretical value of 11 as predicted by previously developed model. The influence of azo bond loading ($L_{\text{azo bond}}$), from 0.25 to 1.0, and pH values from 2.5 to 4.0 were evaluated on AB161 decolorization kinetic rates. A correlation between the natural logarithm of the decolorization rates and $L_{\text{azo bond}}$ was established at the different pH values. The decolorization rate increased linearly with decreasing $L_{\text{azo bond}}$, in the order of pH: 3.5 > 3.0 > 2.5 > 4.0. UV radiation of Fenton processes increases degradation of AB161 more than 40 % due to the regeneration of Fe^{2+} through photo-catalytic reactions. This phenomenon was confirmed by measuring H_2O_2 concentration during the photo-Fenton processes. The results suggest that Fenton processes can effectively decolorize or degrade wastewater containing azo dye, AB161. Photo-Fenton processes may further increase the degradation efficiency of AB161 by 40 %.

Keywords H_2O_2/Fe^{2+} · Photo-Fenton · Oxidation · Kinetics · Azo bond · Chemical oxygen demand

Introduction

Azo, triarylmethane, anthraquinonic, heterocyclic, and phytalocyanine dyes are major groups of commercial dyes. Among these dyes, azo dyes are the largest class used in textile industry and characterized by one or more azo bonds (–N=N–). Most azo dyes are resistant to biodegradation under aerobic conditions and could be toxic to microorganisms and plants if they are discharged without proper treatment (Gupte et al. 2013; Patil and Jadhav 2013; Przytás et al. 2013). Studies in the literature show that advanced oxidation processes (AOPs), which generate hydroxyl radical, can rupture dye chromophore and convert recalcitrant azo dyes into carbon dioxide, water, and inorganic ions (Goi et al. 2010; Zapata et al. 2009, 2010; Lopez et al. 2004; Rameshraja and Suresh 2011; Shafieiyoun et al. 2012; Asaithambi et al. 2014). Among the AOPs studied, Fenton or photo-Fenton process has many advantages because it is a homogeneous process and favors a better contact between reagent species without mass transfer limitation. Several operational parameters such as the concentration of hydrogen peroxide, iron, target compound, pH and temperature can significantly affect the efficiency of the processes. Fenton process uses Fe^{2+} salt and H_2O_2 solution in acid medium (Eq. 1) to produce hydroxyl radicals. The degradation efficiency of azo dyes can be further enhanced by coupling of the Fenton's

---

Communicated by UNITED STATES.

✉ W. Z. Tang
tangz@fiu.edu

[1] Instituto de Química, Universidade Federal de Uberlândia, Uberlândia, MG 38400-902, Brazil

[2] Department of Treatment of Haz-Mat, Environment and Water Resources and Technology Directorate, Ministry of Science and Technology, Baghdad, Iraq

[3] Department of ChemTech, Faculty of Technology, Lappeenranta University of Technology, 53850 Lappeenranta, Finland

[4] Department of Civil and Environmental Engineering, Florida International University, Miami, FL 33174, USA

reagents with UV or solar radiation (Eq. 2), because Fe^{2+} ions are regenerated through reactions (1) and (2) and allow Fenton reaction of Eq. (1) to continue. The coupling of UV and Fenton reaction is generally referred as photo-Fenton process.

$$Fe^{2+} + H_2O_2 \rightarrow Fe^{3+} + {}^{\cdot}OH + OH^- \quad k = 76\ M^{-1}s^{-1} \tag{1}$$

$$Fe(OH)^{2+} + h\nu \rightarrow Fe^{2+} + {}^{\cdot}OH \tag{2}$$

Several azo dyes such as Acid Black 1 (Wang 2008; Chang et al. 2009), Acid Orange 8 and Acid Red 44 (Tunç et al. 2013), Acid Red 66 and Direct Blue 71 (Tunç et al. 2012; Ertugay and Acar 2013), Direct Blue 15 (Sun et al. 2009a), and Procion Red H-E7B (Garcia-Montano et al. 2008) have been decolorized in aqueous solutions by Fenton and photo-Fenton processes. For example, Tunç et al. (2013) observed that the azo functional groups in Acid Orange 8 and Acid Red 44 dyes can be quickly destroyed. However, oxidation of intermediates such as benzene and naphthalene rings proceeded at much slower rate. Garcia-Montano et al. (2008) identified 18 different aromatic intermediates of Procion Red H-E7B, different short-chain carboxylic acids, and heteroatom oxidation products such as NH_4^+, NO_3^-, Cl^-, and SO_4^{2-}. Complete oxidation of Procion Red H-E7B can be expressed by Eq. (3):

$$\begin{aligned} &C_{52}H_{34}O_{26}S_8Cl_2N_{14} + 76.5O_2 \\ &\quad \rightarrow 52CO_2 + 14NO_3^- + 8SO_4^{2-} + 2Cl^- + 32H^+ + H_2O \end{aligned} \tag{3}$$

In Fenton process, hydroxyl radical preferably attacks the chromophore center of the dye molecule (i.e., the azo groups, –N=N–) by cleaving them in three parts: the two lateral substituted groups and the central body. The second attacking center is the chromophore azo bond by producing primary aromatic amines as intermediates and inorganic end product such as NH_4^+ (Lachheb et al. 2002; Karkmaz et al. 2004). To treat textile wastewater containing azo dyes, one objective is to decolorize recalcitrant azo dyes by destroying the chromophore azo bond to improve its biodegradability. Our previous studies reported that azo bonds could be oxidized efficiently by UV/TiO_2 or H_2O_2/iron powder system (Tang and Chen 1996; Tang et al. 1997). After the azo bond was destroyed, the intermediates would be easier to be biodegraded. Another treatment objective is the reduction in the chemical oxygen demand (COD) of the textile wastewater. Usually, these two objectives will require different stoichiometry of chemical reagents such as H_2O_2 and Fe^{2+} according to either azo bond or COD loadings. So far, no study in this aspect has been found on Fenton or photo-Fenton oxidation of azo dye, AB161. Therefore, the present paper reports the decolorization or COD removal kinetics of the azo dye Acid Blue 161 (AB161), which contains one azo bond, by Fenton or photo-Fenton processes.

Optimal operation parameters for either Fenton or photo-Fenton processes depend upon different treatment objectives such as decolorization or COD removal. Therefore, the specific objectives of the present study were: (1) to determine the optimal H_2O_2/Fe^{2+} molar ratio during Fenton oxidation of AB161 at pH 3.5 according to the decolorization kinetics by fixing H_2O_2 while varying Fe^{2+} and vice versa; (2) to evaluate the effects of either azo bond loading factor ($L_{\text{azo bond}}$) or COD loading factor (L_{COD}) at different pH values on the decolorization kinetic rates or COD removal of AB161 by either Fenton or photo-Fenton processes at the optimal molar ratio of H_2O_2/Fe^{2+}; (3) under the best pH, $L_{\text{azo bond}}$, and, molar ratio H_2O_2/Fe^{2+}, to evaluate the correlations between the decolorization kinetic rates and the decolorization efficiencies (η) with the H_2O_2/AB161 molar ratio. This work is conducted in the Department of Civil and Environmental Engineering of Florida International University, Miami, Florida, from November 2013 to February 2014.

Materials and methods

Reagents

All solutions were prepared using deionized water. The AB161 standard (Aldrich) was used as received. H_2O_2 (50 % w/w) and $FeSO_4 \cdot 7H_2O$ (Fischer Scientific), Na_2SO_3 and NaOH (Sigma-Aldrich) were used as received. A solution of ammonium metavanadate (MP Biomedicals) was prepared and used at a concentration of 0.062 M in 0.58 M H_2SO_4 (J.T. Baker) in quantification of H_2O_2 concentration.

Fenton and photo-Fenton experiments

Fenton experiments were carried out by using 1.0 L of AB161 solutions in a 2-L jar test apparatus (Phipps and Bird, Richmond, VA). Mechanical mixing speed was 100 rpm, and room temperature ranged from 18 to 22 °C. The photo-Fenton experiments were conducted by using a Rayonet photochemical reactor (Southern New England Ultraviolet Co., Model RPR-100). Inside the reaction chamber, 17 UV lamps were uniformly distributed around a reactor as described by Tang and An (1995). According to the manufacturer, each lamp supplies 90 % of its output as 350 nm light with an intensity of 9200 W cm^{-2} at the center of the reactor (Tang and An 1995). A beaker of 1 L was placed at the center inside of the chamber with a magnetic stirrer. The cooling air was provided by a fan mounted at the bottom of the photo-reactor to protect the reaction vessel from the hot lamp surface. As a result, temperature inside the chamber was maintained from 18 to 22 °C. The experiments were preceded according to the following procedure:

First, to investigate the effects of the initial H_2O_2 concentration (ranging from 3.7×10^{-5} to 1.8×10^{-2} M) on the decolorization kinetics of AB161 (1.0×10^{-4} M), Fenton experiments were conducted at a fixed Fe^{2+} concentration of 1.0×10^{-4} M and initial pH of 3.5 (without further adjustment). Each experiment was started by addition of the desired amount of $FeSO_4 \cdot 7H_2O$ crystals previously weighed and dissolved separately in a beaker using the same solution contained in the reaction jar for Fenton reaction or the beaker for photo-Fenton reaction. The dissolved $FeSO_4 \cdot 7H_2O$ was then added to the dye solution under the mechanical mixing or magnetic stirring, respectively. After the pH was adjusted to a desired value by using either 1 M H_2SO_4 or 1 M NaOH, the amount of H_2O_2 was calculated according to the predetermined H_2O_2 concentration and was added in a single step to the batch reactor. To monitor the AB161 concentration during the decolorization process, 5 mL of sample aliquots was taken at each 1 min up to 10 min.

Second, experiments on the effects of Fe^{2+} concentration ranged from 5.0×10^{-6} to 4.0×10^{-4} M on decolorization rate of 1.0×10^{-4} M AB161 solution were investigated under the optimal condition of H_2O_2 concentration of 1.1×10^{-3} M at initial pH 3.5 (without further adjustment). Samples were taken at the same time interval as that in the first step.

Third, the optimal molar ratio H_2O_2/Fe^{2+} was experimentally determined by changing either H_2O_2 or Fe^{2+} concentrations, while one factor was changing at one time but keeping the other parameters constant. Experiments were conducted at different initial pH values from 2.5 to 4.0 (without further adjustment) and at different initial $L_{\text{azo bond}}$ for the Fenton process. In the literature, H_2O_2 dose was usually determined by conducting multiple experiments at variable number of doses at different ratios of H_2O_2 to COD (Goi et al. 2010; Lopez-Alvarez et al. 2012). In this study, we hypothesized that the stoichiometric requirements of Fenton's reagent dose should depend upon the amount of available O_2 in H_2O_2 for hydroxyl radical production during the oxidation of azo bond and its organic intermediates. Therefore, the required dose of H_2O_2 should be based on the initial $L_{\text{azo bond}}$, L_{COD} of AB161, and O_2 supplied by H_2O_2, respectively. A maximum $L_{\text{azo bond}}$ and L_{COD} of 1.00 was used in the experiments because it is the minimum theoretical amount of O_2 required to oxidize all the azo bond group and organic matter present in AB161 dye solution (Eqs. 4 and 5). Our approach attempts to establish universal correlation equations between dimensionless parameters such as decolorization efficiencies (η) with loading rate factors such as $L_{\text{azo bond}}$ or L_{COD}, which are defined by Eqs. (4), (5), and (6), respectively:

$$\eta = \left(\frac{\text{Moles AB161}_{\text{removed}}\left(\text{mol L}^{-1}\right)}{\text{O}_{2\,\text{available}}\left(\text{mol L}^{-1}\right)}\right) = \left(\frac{\text{Moles AB161}_{\text{removed}}\left(\text{mol L}^{-1}\right)}{0.5x[\text{H}_2\text{O}_2]\left(\text{mol L}^{-1}\right)}\right) \tag{4}$$

$$L_{\text{azo bond}} = \left(\frac{\text{Moles azo bond}_{\text{initial}}\left(\text{mol L}^{-1}\right)}{\text{O}_{2\,\text{available}}\left(\text{mol L}^{-1}\right)}\right) = \left(\frac{\text{Moles azo bond}_{\text{initial}}\left(\text{mol L}^{-1}\right)}{0.5x[\text{H}_2\text{O}_2]\left(\text{mol L}^{-1}\right)}\right) \tag{5}$$

$$L_{\text{COD}} = \left(\frac{\text{Moles COD}_{\text{initial}}\left(\text{mol L}^{-1}\right)}{\text{O}_{2\,\text{available}}\left(\text{mol L}^{-1}\right)}\right) = \left(\frac{\text{Moles COD}_{\text{initial}}\left(\text{mol L}^{-1}\right)}{0.5x[\text{H}_2\text{O}_2]\left(\text{mol L}^{-1}\right)}\right) \tag{6}$$

where 'available O_2' is the theoretical amount of reactive O_2 equivalent to the added H_2O_2. Theoretically, 1 mol of H_2O_2 has 0.50 mol of available O_2 for oxidation of AB161 as shown in Eq. (7):

$$2H_2O_2 \rightarrow 2H_2O + O_2 \tag{7}$$

Either decolorization or COD removal kinetics of azo dye, AB161, was investigated at different loading factors (1.0, 0.75, 0.50, and 0.25) at a fixed H_2O_2/Fe^{2+} molar ratio of 11, respectively. Molecular structure of AB161 indicates that 1.0×10^{-4} mol of AB161 dye has 1.0×10^{-4} mol of azo group bond. H_2O_2 concentrations evaluated for the destruction of azo group bond were: 2.0×10^{-4}; 2.7×10^{-4}; 4.0×10^{-4}; and 8.0×10^{-4} M. At the experimentally determined optimal initial pH of 3.5 (without further adjustment), H_2O_2/Fe^{2+} molar ratio of 11, the effects of the $L_{\text{azo bond}}$ and L_{COD} on the decolorization kinetics were also evaluated with 1.0×10^{-4} M AB161 solution to compare the Fenton and the photo-Fenton processes. For COD removal of AB161 during L_{COD} experiments, however, different H_2O_2 concentrations (6.4×10^{-3}; 8.5×10^{-3}; 1.3×10^{-2}; 2.6×10^{-2} M) were used, because the experimental COD concentration obtained at 1.0×10^{-4} M AB161 solution was 102 mg O_2 L^{-1} (COD = 3.2×10^{-3} M). Finally, under the optimal conditions for AB161 decolorization: $L_{\text{azo bond}} = 0.25$, $[H_2O_2] = 8.0 \times 10^{-4}$ M, $[Fe^{2+}] = 7.3 \times 10^{-5}$ M and initial pH 3.5 (without further adjustment), the color removal was evaluated at different AB161 concentrations (from 2.5×10^{-5} to 1.5×10^{-4} M) and the correlations between either the decolorization rate constants or the decolorization efficiency (η) with the molar ratio H_2O_2/AB161 were established, respectively.

For the experiments evaluating the AB161 decolorization kinetics, an excess of Na_2SO_3 solution (1 M) was added to the samples before analysis. The added Na_2SO_3 ensures the removal of the residual H_2O_2 by terminating Fenton reactions in the sample. However, for the experiments evaluating the COD removal, the Na_2SO_3 was added according to the stoichiometry between H_2O_2 and Na_2SO_3 and the number of moles of the remaining H_2O_2. This procedure eliminates the interference of Na_2SO_3 on the COD analyses (Vogel et al. 2000).

Analytical methods

AB161 concentration of samples taken during the Fenton or photo-Fenton experiments was determined through measurement of the absorbance at maximum wavelength ($\lambda_{max} = 600$ nm) of AB161 according to the predetermined calibration curve. The COD was determined based on the standard photometric method 5220 D (Clesceri et al. 2005). Hydrogen peroxide was quantified spectrophotometrically as described by Nogueira et al. (2005).

Results and discussion

Influence of H_2O_2 concentration on AB161 decolorization kinetics

H_2O_2 concentration is a determining factor in Fenton oxidation of AB161. Excessive H_2O_2 consumes hydroxyl radicals without the degradation of the targeted organic matter. As a result, the oxidation efficiency of the targeted pollutant by the Fenton process would be reduced (Wang 2008; Tunç et al. 2013). On the other hand, insufficient amount of H_2O_2 could not provide sufficient amount of hydroxyl radicals for the maximal oxidative power. For this reason, the effect of H_2O_2 concentration on the decolorization kinetic of AB161 was evaluated first.

The kinetics of Fenton process can be quite complex due to a great number of reactions simultaneously taking place. Three kinetic models such as the zero order, the first order, and the second order have been used to fit the experimental data points obtained from the decolorization processes. Table 1 shows that the fitting of the zero-order and the first-order models to the experimental data was not good enough due to the low correlation coefficients. However, correlation coefficient values of the second-order model are mostly higher than those of the zero-order and first-order models. In fact, all the experimental data under different reaction conditions are represented well by the second-order model, which suggests that the decolorization kinetics of AB161 follow the second-order kinetics.

The correlations between the AB161 decolorization second-order kinetics and different initial H_2O_2 concentrations (from 3.7×10^{-5} to 1.8×10^{-2} M) (Table 1) are presented in Fig. 1.

Figure 1 presents that the AB161 decolorization kinetic rates at a fixed Fe^{2+} concentration of 1.0×10^{-4} M increase with the H_2O_2 concentration in two different steps: (1) For the lowest dose of H_2O_2 ranged from 3.7×10^{-5} to 1.1×10^{-3} M, the AB161 decolorization kinetics increased sharply with a slope of 3.3×10^5; (2) subsequently, increasing the H_2O_2 from 1.1×10^{-3} to 1.8×10^{-2} M, AB161 decolorization kinetics increases with a lower slope of 6.4×10^4 (Fig. 1a).

The natural logarithms of AB161 concentration during decolorization were plotted against the natural logarithm H_2O_2 concentrations, and a linear correlation between them was established as: $\ln k = 9.6 + 0.57 \times \ln [H_2O_2]$, with a regression coefficient, R^2, of 0.98 (Fig. 1b). The positive effect on the AB161 decolorization kinetics values of the initial H_2O_2 concentration is due to the higher yield of hydroxyl radical. When H_2O_2 concentration was greater than 1.1×10^{-3} M (Fig. 1a), the AB161 decolorization kinetics values increased linearly with the H_2O_2

Table 1 Parameters of kinetic models and correlation coefficients for each H_2O_2 concentration at initial pH 3.5 and 1.0×10^{-4} M Fe^{2+} during Fenton decolorization of 1.0×10^{-4} M AB161

$[H_2O_2]$ (M)	$\frac{[H_2O_2]}{[Fe^{2+}]}$	Zero order		First order		Second order	
		k (M min^{-1})	R^2	k (min^{-1})	R^2	k (M^{-1} min^{-1})	R^2
1.8×10^{-2}	1.8×10^2	4.5×10^{-6}	0.8606	8.0×10^{-2}	0.9455	1.5×10^3	0.9893
8.8×10^{-3}	88	3.5×10^{-6}	0.8875	5.2×10^{-2}	0.9409	7.8×10^2	0.9764
4.4×10^{-3}	44	3.2×10^{-6}	0.9004	4.6×10^{-2}	0.9444	6.5×10^2	0.9753
3.3×10^{-3}	33	2.8×10^{-6}	0.9184	3.8×10^{-2}	0.9510	5.1×10^2	0.9751
1.1×10^{-3}	11	2.1×10^{-6}	0.9317	3.0×10^{-2}	0.9562	4.0×10^2	0.9750
2.2×10^{-4}	2.2	8.9×10^{-7}	0.9655	1.0×10^{-2}	0.9717	1.2×10^2	0.9764
1.1×10^{-4}	1.1	6.6×10^{-7}	0.9567	7.4×10^{-3}	0.9587	8.3×10^1	0.9606
5.5×10^{-5}	0.55	4.6×10^{-7}	0.9362	5.2×10^{-3}	0.9371	5.7×10^1	0.9380
3.7×10^{-5}	0.37	2.7×10^{-7}	0.9026	3.1×10^{-3}	0.9028	3.4×10^{-1}	0.9029

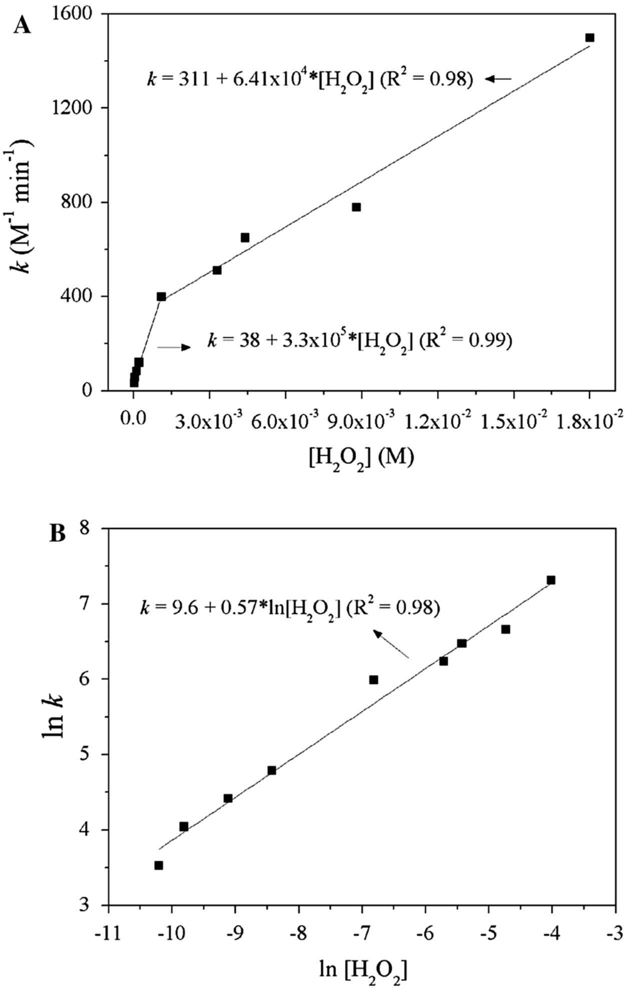

Fig. 1 **a** Direct and **b** natural logarithm correlations between the decolorization rates versus H_2O_2 concentrations used, obtained during AB161 degradation by Fenton process. Initial conditions: [AB161] = 1.0×10^{-4} M; $[Fe^{2+}] = 1.0 \times 10^{-4}$ M and pH 3.5

concentration with lower intensity. It suggests that the overdosed H_2O_2 was scavenging hydroxyl radicals excessively. Therefore, 1.1×10^{-3} M H_2O_2 was chosen as the optimal concentration and used in the next experiments to evaluate the effects of Fe^{2+} concentration on AB161 decolorization kinetics.

Influence of Fe^{2+} concentration on AB161 decolorization kinetics

Fe^{2+} concentration is also an important parameter in Fenton's reactions because it directly influences the yield of hydroxyl radical, ˙OH, by catalytically decomposing H_2O_2 as shown in Eq. (1), while it also would act as scavengers of $^{\bullet}OH$ radicals if it was overdosed (De Laat and Gallard 1999). Therefore, the influence of Fe^{2+} concentration on the AB161 decolorization kinetics was evaluated by fixing the initial H_2O_2 concentration at 1.1×10^{-3} M and initial pH 3.5 (without further adjustment). As an experimental control, in the absence of Fe^{2+} and presence of 1.1×10^{-3} M H_2O_2, there was no AB161 decolorization (Table 2), which demonstrated the important role of the Fe^{2+} in the Fenton process. Table 2 suggests that decolorization of AB161 also followed second-order kinetics for all Fe^{2+} concentrations evaluated, because the higher correlation coefficients for the second-order models were obtained than those for the zero-order and the first-order models.

The correlation between the AB161 decolorization second-order kinetics and the different initial Fe^{2+} concentrations (from 5.0×10^{-6} to 4.0×10^{-4} M) (Table 2) is presented in Fig. 2.

Figure 2 demonstrates that the AB161 decolorization kinetic rates increase with the Fe^{2+} concentration in two different steps also: (1) For the lowest dose of Fe^{2+} ranged from 5.0×10^{-6} to 1.0×10^{-4} M, the AB161 decolorization kinetics increased sharply with a slope of 3.6×10^6; (2) subsequently, increasing the dose of Fe^{2+} (from 1.0×10^{-4} to 4.0×10^{-4} M), AB161 decolorization kinetics increased also with slower slope of 1.9×10^6 (Fig. 2a). The slower decolorization kinetics in the second

Table 2 Parameters of kinetic models and correlation coefficients for each Fe^{2+} concentration at initial pH 3.5 and 1.1×10^{-3} M H_2O_2 during Fenton decolorization of 1.00×10^{-4} M AB161

$[Fe^{2+}]$ (M)	$\frac{[H_2O_2]}{[Fe^{2+}]}$	Zero order		First order		Second order	
		k (M min^{-1})	R^2	k (min^{-1})	R^2	k (M^{-1} min^{-1})	R^2
4.0×10^{-4}	2.8	3.6×10^{-6}	0.8260	5.9×10^{-2}	0.9004	9.8×10^{2}	0.9548
3.0×10^{-4}	3.7	3.3×10^{-6}	0.8711	5.0×10^{-2}	0.9224	8.0×10^{2}	0.9649
1.8×10^{-4}	6.3	2.7×10^{-6}	0.8951	3.9×10^{-2}	0.9344	5.7×10^{2}	0.9640
1.0×10^{-4}	11	2.4×10^{-6}	0.9317	3.0×10^{-2}	0.9562	4.0×10^{2}	0.9750
5.0×10^{-5}	22	1.6×10^{-6}	0.9527	2.1×10^{-2}	0.9653	2.6×10^{2}	0.9758
2.5×10^{-5}	44	1.3×10^{-6}	0.9781	1.6×10^{-2}	0.9841	1.9×10^{2}	0.9888
1.2×10^{-5}	80	6.6×10^{-7}	0.9667	7.7×10^{-3}	0.9692	9.0×10^{1}	0.9715
5.0×10^{-6}	2.2×10^{2}	4.1×10^{-7}	0.9220	4.5×10^{-3}	0.953	5.1×10^{1}	0.9535
0	0	–	–	–	–	–	–

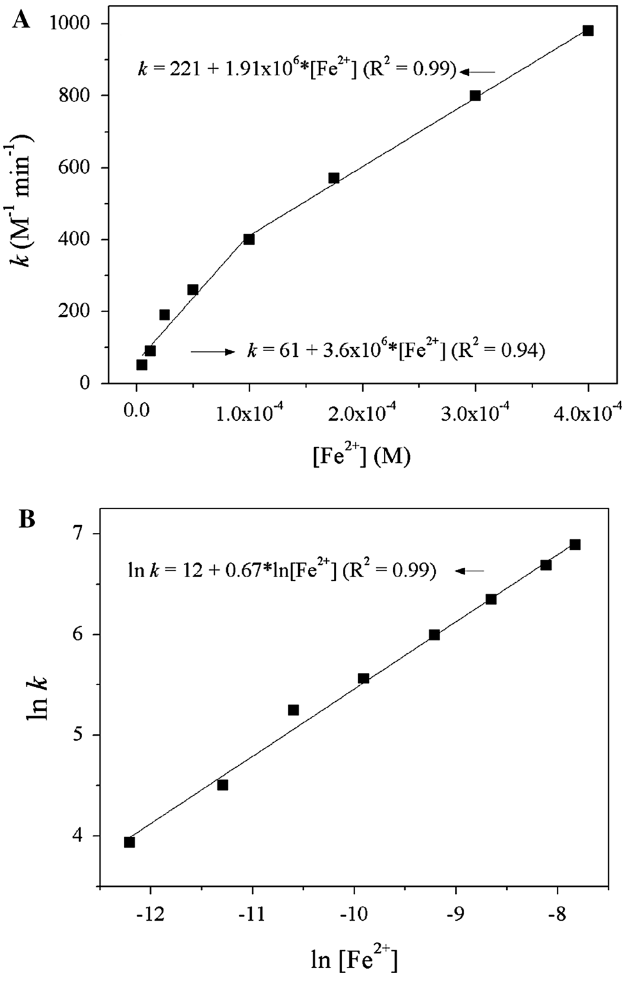

Fig. 2 **a** Direct and **b** natural logarithm correlations between the decolorization rates versus Fe^{2+} concentration used, obtained during AB161 degradation by Fenton process. Initial conditions: $[AB161] = 1.0 \times 10^{-4}$ M; $[H_2O_2] = 1.1 \times 10^{-3}$ M and pH 3.5

phase than the first phase suggests that Fe^{2+} is overdosed by consuming significant amount of hydroxyl radicals in the solution. As a result, the amount of hydroxyl radical available to oxidize AB161 was reduced.

A linear correlation between the AB161 decolorization kinetics and Fe^{2+} concentration was also established by plotting a graphic of the natural logarithm as shown in Fig. 2b. The linear relation was: $\ln k = 12 + 0.67 \times \ln [Fe^{2+}]$, with a regression coefficient, R^2, of 0.99. The positive effect of Fe^{2+} on the AB161 decolorization kinetics confirmed that Fe^{2+} acts as catalyst by rapid decomposition of H_2O_2 into $^{\bullet}OH$ radicals because Fe^{2+} is not able to oxidize organic pollutants. When Fe^{2+} concentration is greater than 1.0×10^{-4} M (Fig. 2a), the AB161 decolorization kinetics rate increased linearly with the Fe^{2+} concentration with lower intensity by scavenging significant amount of hydroxyl radicals. Therefore, 1.0×10^{-4} M Fe^{2+} was chosen as the optimal Fe^{2+} concentration.

Influence of H_2O_2/Fe^{2+} molar ratio on AB161 decolorization kinetics

In Fenton process, the molar ratio of H_2O_2/Fe^{2+} is important since too little iron will result in under-utilized H_2O_2, while the excessive Fe^{2+} acts as scavengers of $^{\bullet}OH$ (Sun et al. 2009b). Since neither H_2O_2 nor Fe^{2+} should be overdosed, it is important to optimize the ratio of H_2O_2 to Fe^{2+}. In theory, for organic compound containing unsaturated azo bond, a transition state complex similar to that hydroxylation of trichloroethylene as proposed by Tang (2004) should also be valid. According to the previous mathematical derivation (Tang 2004), the theoretical H_2O_2/Fe^{2+} molar ratio should be 11 for organic pollutants containing double bond such as trichloroethylene. The numerical value of 11 is the ratio between two second-order rate constants of Eqs. (9)–(8), k_9/k_8, as follows:

$$OH^{\cdot} + H_2O_2 \rightarrow HO_2^{\cdot} + H_2O \quad k_8 = 2.7 \times 10^7\ M^{-1}s^{-1} \tag{8}$$

$$Fe^{2+} + OH^{\cdot} \rightarrow Fe^{3+} + OH^{-} \quad k_9 = 3 \times 10^8\ M^{-1}s^{-1} \tag{9}$$

Since Eqs. (8) and (9) present the consumption of hydroxyl radical by H_2O_2 and Fe^{2+}, respectively, the optimal H_2O_2/Fe^{2+} molar ratio of 11 can be expressed as:

$$\frac{[H_2O_2]}{[Fe^{2+}]}\Big|_{\text{optimal}} = k_9/k_8 \tag{10}$$

Equation (10) simply reflects the fact that the scavenging rate of hydroxyl radical by overdosed H_2O_2 or Fe^{2+} should be at the same rate if the optimal H_2O_2/Fe^{2+} molar ratio were to be maintained:

$$k_8[H_2O_2] = k_9\left[Fe^{2+}\right] \tag{11}$$

When the above condition is satisfied, neither H_2O_2 nor Fe^{2+} concentration is overdosed. As explained by Tang (2004), this optimal condition only applies to organic compound containing unsaturated π bond such as C=C or azo bond (–N=N–) which is contained in AB161 in this study. Therefore, if hydroxyl radical preferably attacks the azo bond (–N=N–), the optimal H_2O_2/Fe^{2+} molar ratio during decolorization of AB161 should be also equal 11. However, literature values show that the optimal molar ratio of H_2O_2/Fe^{2+} was different for decolorization of different azo dyes. For example, optimal molar ratio of H_2O_2/Fe^{2+} was 30:1 and 15:1 at 25 °C and pH 3.5 for 2.9×10^{-5} M Acid Orange 8 and Acid Red 44, respectively (Tunç et al. 2013), and, 100:1 at 30 °C and pH 4.0 for 4.7×10^{-5} M Direct Blue 15 (Sun et al. 2009a). These differences may very likely suggest that different oxidation mechanisms exist during the Fenton oxidation of different azo dyes.

To find out the optimal molar ratio of H_2O_2/Fe^{2+} during the decolorization of AB161, first, the concentration of Fe^{2+} was kept constant at 1.0×10^{-4} M, and the amount of H_2O_2 was varied so that the H_2O_2/Fe^{2+} molar ratio ranged from 0.37 to 1.8×10^{2} which is listed in Table 1; second, H_2O_2 was maintained constant at 1.1×10^{-3} M, and the amount of Fe^{2+} was varied so that the H_2O_2/Fe^{2+} molar ratio ranged from 2.8 to 2.2×10^{2} as shown in Table 2. The experimental AB161 decolorization kinetics values for the H_2O_2/Fe^{2+} molar ratios tested are shown in Fig. 3a.

Figure 3a shows that decolorization rate constant k at the fixed Fe^{2+} concentration of 1.0×10^{-4} M increases with increasing H_2O_2/Fe^{2+} molar ratio, while it decreases with increasing H_2O_2/Fe^{2+} molar ratio when H_2O_2 concentration was fixed at 1.1×10^{-3} M. The two curves intersected at about 12, which reasonably agree with the theoretically predicted value of 11. To further quantify the optimal ratio H_2O_2/Fe^{2+} for the system, a linear correlation was established by plotting the natural logarithm of the decolorization kinetic values as a function of the natural logarithm of the H_2O_2/Fe^{2+} molar ratio values as shown in Fig. 3b. Two linear correlation equations were established. When Fe^{2+} concentration was fixed at 1.0×10^{-4} M, the oxidation rate constant of AB161 increased with H_2O_2/Fe^{2+} molar ratio as follows:

$$\ln k = 4.3 + 0.57 \times \ln \frac{H_2O_2}{Fe^{2+}} \tag{12}$$

When H_2O_2 concentration was fixed at 1.1×10^{-3} M, the oxidation rate constant of AB161 decreased with H_2O_2/Fe^{2+} molar ratio as follows:

$$\ln k = 7.6 - 0.67 \times \ln \frac{H_2O_2}{Fe^{2+}} \tag{13}$$

At the optimal H_2O_2/Fe^{2+} molar ratio, the right-hand side of Eqs. (12) and (13) should be equal. The solution of the two equations gave the analytically derived optimal H_2O_2/Fe^{2+} molar ratio of 14.30, which is the intercept of the two straight lines in Fig. 3b. Again, it reasonably agrees with the theoretically predicted value of 11. Therefore, the theoretically optimal H_2O_2/Fe^{2+} molar ratio of 11 was chosen as the best condition and was used in the next experiments to evaluate the effects of pH, $L_{\text{azo bond}}$, L_{COD}, and AB161 concentration, on decolorization or COD removal of AB161 dye by Fenton and photo-Fenton processes.

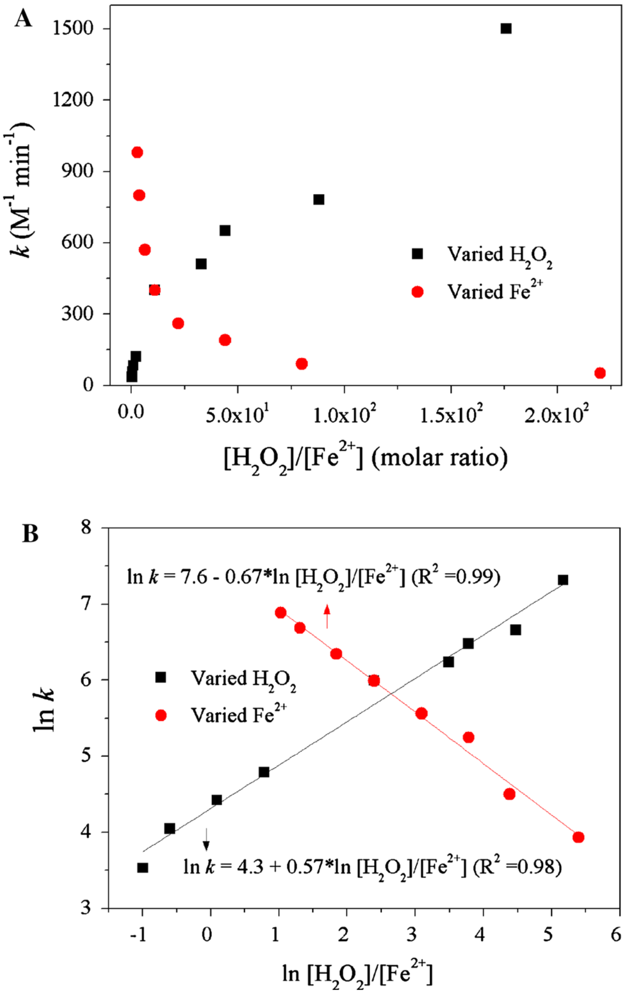

Fig. 3 **a** Direct and **b** natural logarithm correlations between the decolorization rates versus H_2O_2/Fe^{2+} molar ratio used, obtained during AB161 degradation by Fenton process, keeping Fe^{2+} constant and ranging H_2O_2, and, vice versa. Initial conditions: $[AB161] = 1.0 \times 10^{-4}$ M; $[Fe^{2+}] = 1.0 \times 10^{-4}$ M; $[H_2O_2] = 1.1 \times 10^{-3}$ M and pH 3.5

Influence of pH and $L_{\text{azo bond}}$ on AB161 decolorization kinetics

pH strongly affects the degradation efficiency in Fenton process, since a change of the solution pH involves a variation of the concentration of Fe^{2+} species and consequently the production rate of $^{\bullet}OH$ radicals responsible for oxidation of AB161 (Nogueira et al. 2007; Machulek et al. 2012). Parallel experiments were conducted at four initial pH values (2.5, 3.0, 3.5, and 4.0) (without further adjustment). Since increasing the Fenton's reagents (H_2O_2 and Fe^{2+}) increases the generation of hydroxyl radicals, which are responsible for the dye degradation, the influence of four $L_{\text{azo bond}}$ factor values (0.25, 0.50, 0.75, and 1.0) at fixed molar ratio H_2O_2/Fe^{2+} of 11 was evaluated. All the experimental data at four pH levels are also represented well by the second-order model as shown in Table 3. A significant difference in AB161 decolorization rates at each pH and $L_{\text{azo bond}}$ was observed.

Table 3 Second-order kinetic constants and correlation coefficients for each initial pH and $L_{\text{azo bond}}$ value during Fenton decolorization of 1.0×10^{-4} M AB161

pH	$L_{\text{azo bond}}$			
	1.0	0.75	0.50	0.25
2.5*	$k = 68$ M^{-1} min^{-1} $R^2 = 0.96$	$k = 109$ M^{-1} min^{-1} $R^2 = 0.94$	$k = 191$ M^{-1} min^{-1} $R^2 = 0.86$	$k = 425$ M^{-1} min^{-1} $R^2 = 0.88$
3.0*	$k = 71$ M^{-1} min^{-1} $R^2 = 0.96$	$k = 119$ M^{-1} min^{-1} $R^2 = 0.95$	$k = 224$ M^{-1} min^{-1} $R^2 = 0.95$	$k = 722$ M^{-1} min^{-1} $R^2 = 0.96$
3.5*	$k = 66$ M^{-1} min^{-1} $R^2 = 0.95$	$k = 112$ M^{-1} min^{-1} $R^2 = 0.88$	$k = 258$ M^{-1} min^{-1} $R^2 = 0.88$	$k = 731$ M^{-1} min^{-1} $R^2 = 0.90$
3.5$^{\#}$	$k = 89$ M^{-1} min^{-1} $R^2 = 0.95$	$k = 180$ M^{-1} min^{-1} $R^2 = 0.96$	$k = 256$ M^{-1} min^{-1} $R^2 = 0.99$	$k = 1287$ M^{-1} min^{-1} $R^2 = 0.99$
4.0*	$k = 46$ M^{-1} min^{-1} $R^2 = 0.91$	$k = 66$ M^{-1} min^{-1} $R^2 = 0.94$	$k = 147$ M^{-1} min^{-1} $R^2 = 0.90$	$k = 406$ M^{-1} min^{-1} $R^2 = 0.87$

* Fenton, $^{\#}$ photo-Fenton

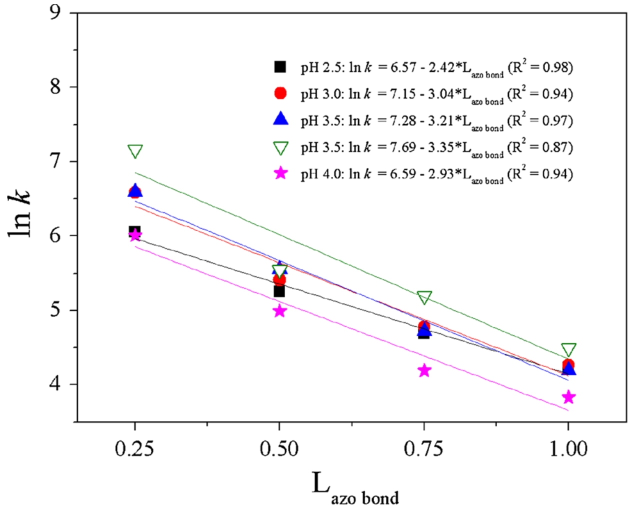

Fig. 4 Correlation between the natural logarithm of the decolorization rates versus $L_{\text{azo bond}}$ to different pH values obtained during 1.0×10^{-4} M AB161 degradation by Fenton (*solid symbols*) and photo-Fenton processes (*open symbols*)

Table 3 shows that the best decolorization rates of AB161 occurred at the initial pH values of 3.5 and 3.0, followed by 2.5 and 4.0. These results are in agreement with the work evaluating the decolorization of Acid Orange 8 and Acid Red 44 (Tunç et al. 2013). The lower k values at the corresponding low and high pH values can be attributed to the lower reaction rate of $[Fe(H_2O)]^{2+}$, scavenging of $^{\cdot}OH$ by H^+, and deactivation of iron ions into iron oxyhydroxides (Nogueira et al. 2007; Machulek et al. 2012). Moreover, the best AB161 decolorization rates were obtained at the lowest $L_{\text{azo bond}}$ factor of 0.25, because the lower $L_{\text{azo bond}}$ factor stands for a higher amount of H_2O_2 concentration per mole of AB 161 and corresponds to the higher O_2 concentration available for oxidizing the AB161 azo dye. In addition, when the molar ratio H_2O_2/Fe^{2+} was fixed at 11, the higher amount of hydroxyl radicals would be produced by higher Fe^{2+} concentrations at the lower $L_{\text{azo bond}}$ value. Therefore, the AB161 decolorization removal rate increases with decreasing $L_{\text{azo bond}}$ at all pH values evaluated. A linear correlation was established between the natural logarithm of the k values and the $L_{\text{azo bond}}$ at each pH value evaluated. The correlation coefficients obtained were higher than 0.87 (Fig. 4). Since there was no significant difference in terms of decolorization rate at pH 3.0 and 3.5, pH of 3.5 was chosen to be used in the next set of experiments to compare the Fenton and the photo-Fenton processes.

Comparison between Fenton and photo-Fenton processes for decolorization or COD removal of AB161 at different $L_{\text{azo bond}}$ and L_{COD} factors

The combination of UV radiation and Fenton's reagent is a promising AOP for the treatment of wastewaters containing azo dyes, since UV light promotes the photo-decarboxylation of ferric carboxylates, reduces ferric to ferrous iron, and yields additional hydroxyl radical by photolysis (Nogueira et al. 2007). This could significantly reduce the amount of sludge due to lower amount of iron required (Hermosilla et al. 2009). Therefore, under the best pH of 3.5 which was determined previously, experiments using four different $L_{\text{azo bond}}$ and L_{COD} values (0.25, 0.50, 0.75, and 1.0) were carried out to investigate the efficiency of either Fenton or photo-Fenton processes on the decolorization or COD removal kinetics of AB161 by these two processes, respectively.

For the AB161 decolorization rates by both processes, only slight positive effect of the present UV radiation was observed, except at the lower $L_{\text{azo bond}}$ of 0.25, where a significant positive effect exists (Table 3; Fig. 4). The insignificant effect of UV radiation on the Fenton process (photo-Fenton process) on AB161 decolorization rates at the high $L_{\text{azo bond}}$ evaluated (1.0, 0.75 and 0.50) can be attributed to the strong intensity of the blue color of the initial 1.0 × 10^{-4} M AB161 solution. The high dye concentration severely hinders UV light transmission through the solution. As a result, the photoreduction of Fe^{3+} to Fe^{2+}, which is strongly dependent on the intensity of the radiation and the speciation of ferric ion, was greatly inhibited. This result is in agreement with the control experiment carried out in absence of Fe^{2+} and H_2O_2, where a photodegradation lower than 5 % of the initial 1.0 × 10^{-4} M AB161 solution was obtained, due the strong intensity of the blue color. However, a significant difference between the two processes on decolorization rates using the lower $L_{\text{azo bond}}$ was observed, due to the higher decolorization efficiency, reducing the strong blue color, and favoring the photo-Fenton over the conventional Fenton process.

The different kinetics during the COD removal of AB161 by the Fenton and the photo-Fenton processes is shown in Fig. 5a. For both processes, the COD removal increases with decreasing L_{COD}. However, for Fenton process, at the minimum ($L_{\text{COD}} = 1.0$) and four times ($L_{\text{COD}} = 0.25$) the theoretical amount of the concentration of H_2O_2 to complete removal of COD, only 29 and 48 % of COD removal were achieved after 10 min, respectively (Fig. 5a). These results demonstrate that although there was residual H_2O_2 in solution after 10 min of Fenton's reaction (Fig. 5b), probably all the ferrous iron was converted to ferric ion, reducing the reaction rate with H_2O_2, since a slower consumption of H_2O_2 was observed (Fig. 5b).

On the other hand, when H_2O_2 was at the theoretical minimum amount ($L_{\text{COD}} = 1.0$), 64 and 77 % of COD removal were reached after 1 and 10 min, respectively, using the photo-Fenton process (Fig. 5a). The higher efficiency of the photo-Fenton than Fenton process can be easily explained by the highly positive UV radiation effect. Using the L_{COD} 1.00, a higher amount of H_2O_2 was used compared with the experiments at $L_{\text{azo bond}}$ of 1 (as described in Sect. 2.2) and consequently a higher amount of Fe^{2+}, when the initial H_2O_2/Fe^{2+} molar ratio was fixed at 11. Therefore, the higher amount of $^{\bullet}OH$ radicals at high Fe^{2+} concentration was generated than that at the low Fe^{2+} concentration, which resulted in the loss of the color in less than 30 s. So, for these experiments, the presence of UV radiation contributed to the reduction in ferric to ferrous iron, establishing a cycle of the Fenton reaction and strongly increasing the COD removal efficiency (Fig. 5a). The results of consumption of H_2O_2 demonstrate that for all photo-Fenton experiments, the H_2O_2 was consumed after 10 min due to Fenton reaction, while only about 50 % H_2O_2 was consumed during the Fenton experiments (Fig. 5b).

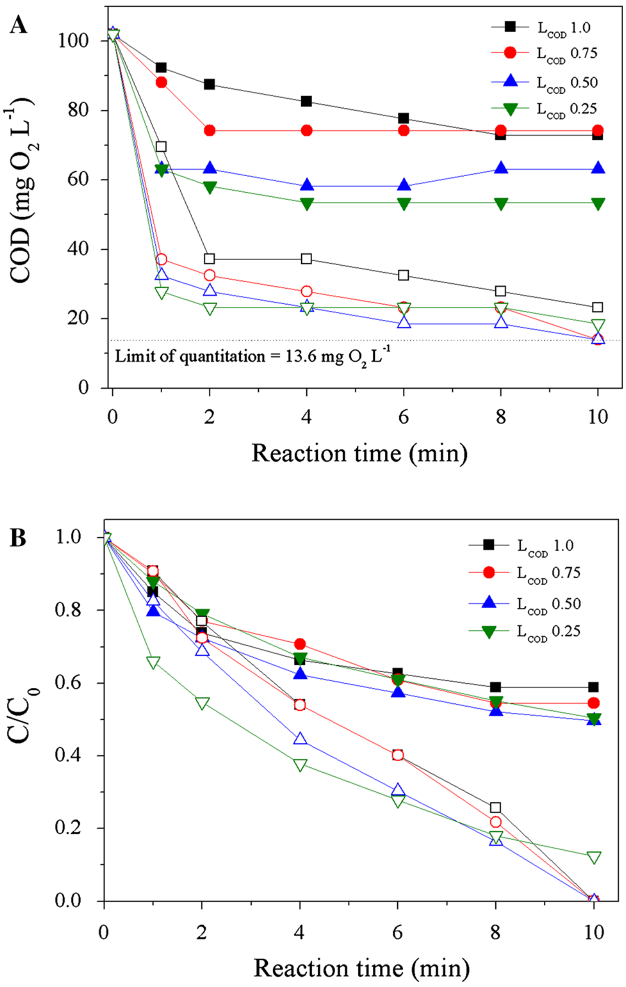

Fig. 5 Comparison of Fenton (*solid symbols*) and photo-Fenton (*open symbols*) on the **a** COD removal of 1.0 × 10^{-4} M AB161 (COD = 102 mg O_2 L^{-1} or 3.2 × 10^{-3} M), and **b** consumption of H_2O_2 using different L_{COD} factors under the best pH 3.5 and molar ratio H_2O_2/Fe^{2+} 11

Influence of AB161 concentration on decolorization kinetics

For practical applications of wide range of textile wastewater containing AB161, the required amount of oxidant, H_2O_2, should depend upon the initial concentration of the azo dye. To establish this dependence quantitatively, investigation has been designed at different initial AB161 concentrations by fixing the initial H_2O_2/Fe^{2+} molar ratio, $L_{\text{azo bond}}$, and pH at 11, 0.25 and 3.5, respectively. Table 4 lists the second-order rate constants of AB161 degradation at the different AB161 concentrations.

Figure 6a shows the effect of different H_2O_2/dye ratios as a function of the decolorization kinetics of AB161. It is evident that the decolorization kinetics increase with the decrease in AB161 concentration in two different steps. A slight increase in decolorization kinetics (from 233 to

Table 4 Second-order kinetic constants and correlation coefficients for each AB161 concentration evaluated at initial pH 3.5, 7.3×10^{-5} M Fe^{2+}, and 8.0×10^{-4} M H_2O_2 during Fenton decolorization

AB161 (M)	$\frac{[H_2O_2]}{[AB161]}$	k (M^{-1} min^{-1})	R^2
1.5×10^{-4}	5.3	233	0.88
1.0×10^{-4}	8.0	731	0.90
6.7×10^{-5}	12	2348	0.95
5.0×10^{-5}	16	5606	0.98
3.3×10^{-5}	24	12,062	0.97
2.5×10^{-5}	32	19,952	0.97

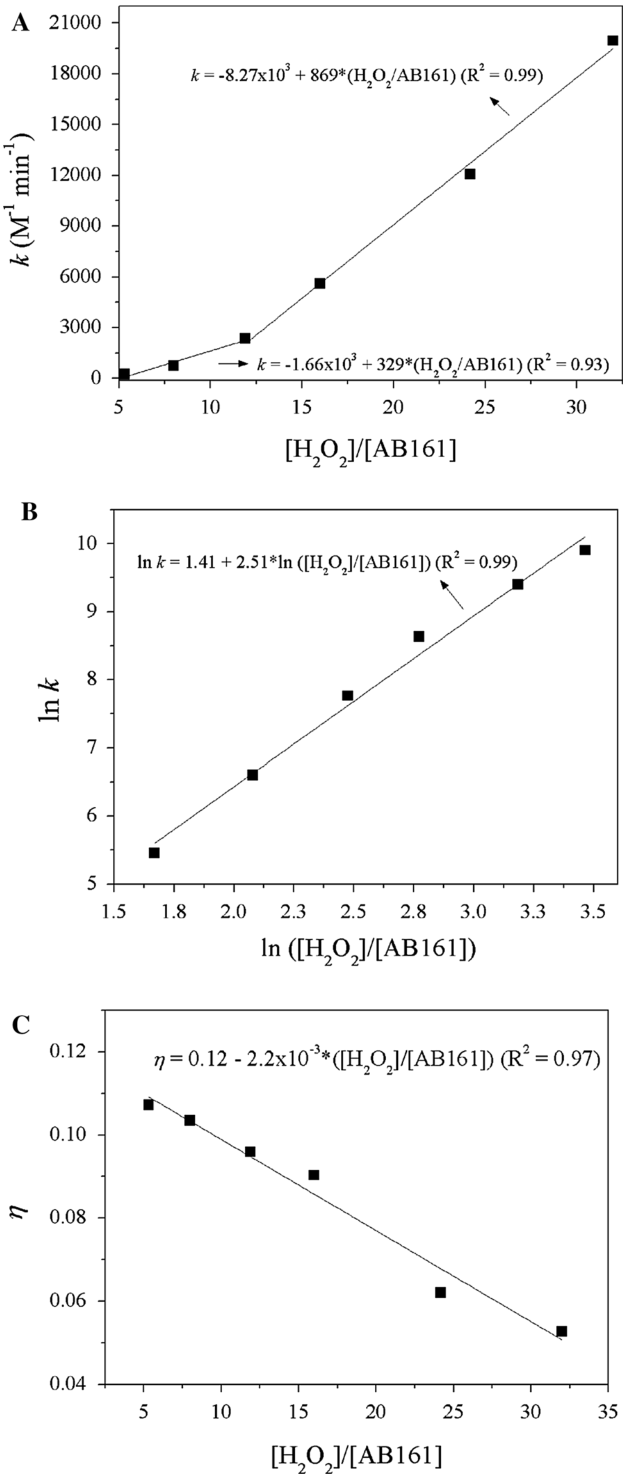

Fig. 6 Correlations between the **a** decolorization rates versus H_2O_2/AB161 molar ratio, **b** natural logarithm of decolorization rates versus natural logarithm of H_2O_2/AB161 molar ratio, and **c** decolorization efficiency versus H_2O_2/AB161 molar ratio, obtained during AB161 degradation by Fenton process at H_2O_2/Fe^{2+} molar ratio 11 and $L_{\text{azo bond}}$ 0.25. Initial conditions: $[Fe^{2+}] = 7.3 \times 10^{-5}$ M; $[H_2O_2] = 8.0 \times 10^{-4}$ M and pH 3.5

2348 M^{-1} min^{-1}) occurred when the H_2O_2/dye ratio increases from 5.3 to 12, with a slope of 329. However, increasing the H_2O_2/dye ratio from 12 to 32, there was a sharp increase in decolorization kinetics (from 2348 to 19,952 M^{-1} min^{-1}). A linear relationship was established by plotting the natural logarithm of the decolorization kinetics rates versus the natural logarithm of the H_2O_2/AB161 molar ratio. The decolorization kinetics rate constants increase with the H_2O_2/AB161 molar ratio (Fig. 6b). On the other hand, the efficiency of AB161 decolorization, η, as defined by Eq. 4 increases with decreasing H_2O_2/AB161 molar ratio (Fig. 6c), which indicates that a higher amount of AB161 was removed by using smaller amount of H_2O_2.

Conclusion

From the experimental data presented in this paper, one of the most important conclusions is that the optimal H_2O_2/Fe^{2+} molar ratio was experimentally determined to be 12 according to the analytical and graphic methods presented in the paper. This ratio reasonably agrees with the theoretically predicted optimal ration of 11 for trichloroethylene, in which only one double bond is available for hydroxyl radical to attack. Since AB161 contains not only the azo bond but also two hydroxylated biphenyl group, several sites may be under hydroxyl radical attack. As a result, the optimal H_2O_2 molar concentration would be higher than theoretically predicted in the TCE (Walter, it is necessary to define TCE) model. The multi-hydroxylation mechanism apparently also contributed to the inverse relationship between the decolorization and COD removal efficiencies with the loading factors.

The decolorization rate of AB161 increased with decreasing $L_{\text{azo bond}}$ factors in the pH sequence:

3.5 > 3.0 > 2.5 > 4.0. An increase in the AB161 azo dye concentration leads to a decrease in the rate of dye decolorization; however, higher efficiency of AB161 decolorization was obtained with increasing the AB161 concentration. The coupling of UV radiation with the Fenton process (photo-Fenton process) enhanced the decolorization rate less than the degree on the COD removal of AB161. These results demonstrate the viability of application of Fenton and photo-Fenton processes in the decolorization or COD removal of wastewater containing azo dye, AB161. More importantly, the dimensionless correlation equations developed in this study may be used to predict the dose required for H_2O_2 and Fe^{2+} under different loading factors such as $L_{\mathrm{azo\ bond}}$ to achieve different degrees of decolorization or L_{COD} for COD removal.

Acknowledgments A. G. Trovó is particularly indebted to CNPq (Conselho Nacional de Desenvolvimento Científico e Tecnológico—Brasil) for the scholarship (Process number: 240990/2012-9). A. K. Hassan would like to thank the Iraq Science Fellowship Program sponsored by the Department of State of the USA and managed by the CRDF Global for all the financial and administrative support.

References

Asaithambi P, Saravanathamizhan R, Matheswaran M (2014) Comparison of treatment and energy efficiency of advanced oxidation processes for the distillery wastewater. Int J Environ Sci Technol. doi:10.1007/s13762-014-0589-9

Chang S-H, Chuang S-H, Li H-C, Liang H-H, Huang L-C (2009) Comparative study on the degradation of I.C. Remazol Brilliant Blue R and I.C. Acid Black 1 by Fenton oxidation and Fe^0/air process and toxicity evaluation. J Hazard Mater 166:1279–1288. doi:10.1016/j.jhazmat.2008.12.042

Clesceri LS, Greenberg AE, Eaton AD (2005) Standard methods for examination of water & wastewater. American Public Health Association (APHA), American Water Works Association (AWWA) & Water Environment Federation (WEF), Washington

De Laat J, Gallard H (1999) Catalytic decomposition of hydrogen peroxide by Fe(III) in homogeneous aqueous solution: mechanism and kinetic modeling. Environ Sci Technol 33:2726–2732. doi:10.1021/es981171v

Ertugay N, Acar FN (2013) Removal of COD and color from Direct Blue 71 azo dye wastewater by Fenton's oxidation: kinetic study. Arabian J Chem. doi:10.1016/j.arabjc.2013.02.009

Garcia-Montano J, Torrades F, Pérez-Estrada LA, Oller I, Malato S, Maldonado MI, Peral J (2008) Degradation pathways of the commercial reactive azo dye Procion Red H-E7B under solar-assisted photo-Fenton reaction. Environ Sci Technol 42:6663–6670. doi:10.1021/es800536d

Goi A, Veressinina Y, Trapido M (2010) Fenton process for landfill leachate treatment: evaluation of biodegradability and toxicity. J Environ Eng 136:46–53. doi:10.1061/(ASCE)EE.1943-7870.0000132

Gupte S, Keharia H, Gupte A (2013) Toxicity analysis of azo Red BS and Methyl Red dye solutions on earthworm (Pheretima phosthuma), micro-organisms, and plants. Desalin Water Treat 51:4556–4565. doi:10.1080/19443994.2012.748637

Hermosilla D, Cortijo M, Huang CP (2009) Optimizing the treatment of landfill leachate by convention Fenton and photo-Fenton processes. Sci Total Environ 407:3473–3481. doi:10.1016/j.scitotenv.2009.02.009

Karkmaz M, Puzenat E, Guillard C, Herrmamm JM (2004) Photocatalytic degradation of the alimentary azo dye amaranth. Mineralization of the azo group of nitrogen. Appl Catal B 51:183–194. doi:10.1016/j.apcatb.2004.02.009

Lachheb H, Puzenat E, Houas A, Ksibi M, Elaloui E, Guillard C, Herrmann JM (2002) Photocatalytic degradation of various types of dyes (Alizarin S, Crocein Orange G, Methyl Red, Cong Red, Methylene blue) in water by UV-irradiated titania. Appl Catal B 39:75–92. doi:10.1016/S0926-3373(02)00078-4

Lopez A, Pagano M, Volpe A, Di Pinto AC (2004) Fenton's pre-treatment of mature landfill leachate. Chemosphere 54:1005–1010. doi:10.1016/j.chemosphere.2003.09.015

Lopez-Alvarez B, Torres-Palma RA, Ferraro F, Penuela G (2012) Solar photo-Fenton treatment of carbofuran: analysis of mineralization, toxicity, and organic by-products. J Environ Sci Health A Toxic Hazard Subst Environ Eng 47:2141–2150. doi:10.1080/10934529.2012.696029

Machulek A Jr, Quina FH, Gozzi F, Silva VO, Friedrich LC, Moraes JEF (2012) Fundamental mechanistic studies of the photo-Fenton reaction for the degradation of organic pollutants. In: Puzyn T, Mostrag-Szlichtyng A (eds) Organic pollutants ten years after the Stockholm convention - environmental and analytical update. In Tech, Rijeka, pp 271–292

Nogueira RFP, Oliveira MC, Paterlini WC (2005) Simple and fast spectrophotometric determination of H_2O_2 in photo-Fenton reactions using metavanadate. Talanta 66:86–91. doi:10.1016/j.talanta.2004.10.001

Nogueira RFP, Trovó AG, da Silva MRA, Villa RD (2007) Fundamentals and environmental applications of Fenton and photo-Fenton processes. Quim Nova 30:400–408. doi:10.1590/S0100-40422007000200030

Patil AV, Jadhav JP (2013) Evaluation of phytoremediation of *Tagetes patula* L. for the degradation of textile dye Reactive Blue 160 and assessment of the toxicity of degraded metabolites by cytogenotoxicity. Chemosphere 92:225–232. doi:10.1016/j.chemosphere.2013.01.089

Przystás W, Zablocka-Godlewska E, Grabinska-Sota E (2013) Effectiveness of dyes removal by mixed fungal cultures and toxicity of their metabolites. Water Air Soil Pollut 224:1534. doi:10.1007/s11270-013-1534-0

Rameshraja D, Suresh S (2011) Treatment of tannery wastewater by various oxidation and combined processes. Int J Environ Res 5:349–360

Shafieiyoun S, Ebadi T, Nikazar M (2012) Treatment of landfill leachate by Fenton process with nano sized zero valent iron particles. Int J Environ Res 6:119–128

Sun J-H, Shi S-H, Lee Y-F, Sun S-P (2009a) Fenton oxidative decolorization of the azo dye Direct Blue 15 in aqueous solution. Chem Eng J 155:680–683. doi:10.1016/j.cej.2009.08.027

Sun SP, Li CJ, Sun JH, Shi SH, Fan MH, Zhou Q (2009b) Decolorization of an azo dye Orange G in aqueous solution by Fenton oxidation process: effect of system parameters and kinetic study. J Hazard Mater 161:1052–1057. doi:10.1016/j.jhazmat.2008.04.080

Tang WZ (2004) Physicochemical treatment of hazardous wastes. Lewis Publishers, Boca Raton

Tang WZ, An H (1995) UV/TiO2 photolytic oxidation of commercial dyes in aqueous solutions. Chemosphere 31:4157–4170. doi:10.1016/0045-6535(95)80015-D

Tang WZ, Chen RZ (1996) Degradation kinetics and mechanisms of commercial dyes by H_2O_2/Iron powder system. Chemosphere 32:947–958. doi:10.1016/0045-6535(95)00358-4

Tang WZ, Zhang Z, An H, Quitana MO, Torres DF (1997) TiO_2/UV photodegradation of azo dyes in aqueous solutions. Environ Technol 18:1–12. doi:10.1080/09593330.1997.9618466

Tunç S, Gürkan T, Duman O (2012) On-line spectrophotometric method for the determination of optimum operation parameters on the decolorization of Acid Red 66 and Direct Blue 71 from aqueous solution by Fenton process. Chem Eng J 181–182:431–442. doi:10.1016/j.cej.2011.11.109

Tunç S, Duman O, Gürkan T (2013) Monitoring the decolorization of Acid Orange 8 and Acid Red 44 from aqueous solution using Fentońs reagents by online spectrophotometric method: effect of operation parameters and kinetic study. Ind Eng Chem Res 52:1414–1425. doi:10.1021/ie302126c

Vogel F, Harf J, Hug A, von Rohr PR (2000) The mean oxidation number of carbon (MOC)—a useful concept for describing oxidation processes. Water Res 34:2689–2702. doi:10.1016/S0043-1354(00)00029-4

Wang S (2008) A comparative study of Fenton and Fenton-like reaction kinetics in decolourisation of wastewater. Dyes Pigm 76:714–720. doi:10.1016/j.dyepig.2007.01.012

Zapata A, Velegraki T, Sánchez-Pérez JA, Mantzavinos D, Maldonado MI, Malato S (2009) Solar photo-Fenton treatment of pesticides in water: effect of iron concentration on degradation and assessment of ecotoxicity and biodegradability. Appl Catal B 88:448–454. doi:10.1016/j.apcatb.2008.10.024

Zapata A, Oller I, Sirtori C, Rodríguez A, Sánchez-Pérez JA, López A, Mezcua M, Malato S (2010) Decontamination of industrial wastewater containing pesticides by combining large-scale homogeneous solar photocatalysis and biological treatment. Chem Eng J 160:447–456. doi:10.1016/j.cej.2010.03.042